Materials Research Proceedings **32** (2023) 235-243 https://doi.org/10.21741/9781644902615-27

In-situ heating observations on microstructure relaxation of ultrafine-grained high-entropy alloys using neutron diffraction and laser-scanning confocal microscopy

Megumi Kawasaki[1,a*], Jae-Kyung Han[1,b], Suk-Chun Moon[2,c], Klaus-Dieter Liss[2,d]

[1] School of Mechanical, Industrial and Manufacturing Engineering, Oregon State University, Corvallis, OR 97331, U.S.A.

[2] School of Mechanical, Materials, Mechatronic and Biomedical Engineering, University of Wollongong, NSW 2522, Australia

[a,]megumi.kawasaki@oregonstate.edu, [b] hanja@oregonstate.edu, [c] scmoon@uow.edu.au, [d] kdl@uow.edu.au

Keywords: High-Pressure Torsion, Laser-Scanning Confocal Microscopy, Nanostructure, Neutron Diffraction, X-Ray Diffraction

Abstract. The thermal stability of ultrafine-grained metals can be fully understood when observing time-resolved microstructural changes over multiple-length scales. The global microstructural relaxation behavior upon heating of an ultrafine-grained (UFG) CoCrFeNi high-entropy alloy (HEA) was characterized by in-situ heating neutron diffraction measurements. Before heating, the nanocrystalline microstructure was introduced by applying high-pressure torsion (HPT), leading to severe lattice distortion by excess dislocations and defects. The sequential information on the structural relaxation of recovery, recrystallization, and grain growth are identified by in-situ heating neutron diffraction analysis defining the texture development, linear thermal lattice expansion, and stress relaxation behaviors of the UFG HEA with increasing temperature up to 1300K. By contrast, nanocrystalline metals processed by HPT are often inhomogeneous microstructurally and compositionally. The influence of such inhomogeneity on the macro-scale microstructural relaxation is monitored using an HPT-processed CoCrFeNiMn high-entropy alloy through in-situ heating laser-scanning confocal microscopy. This study emphasizes the importance of characterization techniques for further in-depth exploration of the SPD-processed ultrafine-grained structure.

Introduction

The thermal stability of metallic materials is a critical ability and design characteristic that can decide the specific applications of engineering metals. It is especially important for ultrafine-grained (UFG) metals and bulk nanostructured materials, whose stored free energy at the grain boundaries is high leading to accelerated microstructural recovery and grain growth [1,2]. Such changes in microstructure directly influence the mechanical properties, i.e., deterioration of strength and hardness, of UFG metals. Thus, the understanding of thermal behavior including microstructural evolution and changes in mechanical properties is significantly important along with the successful development of severe plastic deformation (SPD) techniques for microstructural refinement of numerous metals including multiple-principal element alloys often called high entropy alloy (HEA) [3]. This study describes a recent result on the *in-situ* heating microstructural relaxation behavior of a nanostructured CoCrFeNi alloy examined using neutron diffraction. Moreover, the direct observation of the relaxation microstructure at large length scales is demonstrated on a nanocrystalline CoCrFeNiMn alloy through the application of high-temperature laser-scanning confocal microscopy.

Materials Research Proceedings **32** (2023) 235-243 https://doi.org/10.21741/9781644902615-27

Formation of nanostructure

The present study uses the CoCrFeNi alloy produced by additive manufacturing (AM) of the powder bed fusion technology. The detailed conditions for AM are described earlier [4]. After machining to have disk samples having 10 mm diameter and 0.85 mm thickness, where the disk surfaces are perpendicular to the building direction, high-pressure torsion (HPT) processing was applied to the first batch of the as-built alloy disks for 1/2, 1, 2, 4 and 8 turns under 6 GPa at room temperature. Figure 1 shows the micrographs of the alloy after AM at (a) normal to the built direction and (b) the mid-radius of the disk sample after HPT for 8 turns [5]. The as-built microstructure shows a coarse, columnar grain microstructure. The HPT process refined the microstructure to have reasonably equiaxed grains with an average grain size of d = 90 nm. The microstructural changes during HPT processing occur gradually with increasing numbers of turns, and it is confirmed by taking the hardness contour maps across the disk cross-sections as shown in Fig. 1(c). The initial Vickers microhardness values before HPT was H_V = 260. Due to the imposed shear strain by torsion being proportional to the disk radius [6], high hardness, thus grain refinement, is developed from the disk periphery towards the disk center with increasing HPT turns, while the hardness is homogeneously developed across the disk height. After 8 turns, the hardness distribution became homogeneous in the nanostructured AM CoCrFeNi alloy.

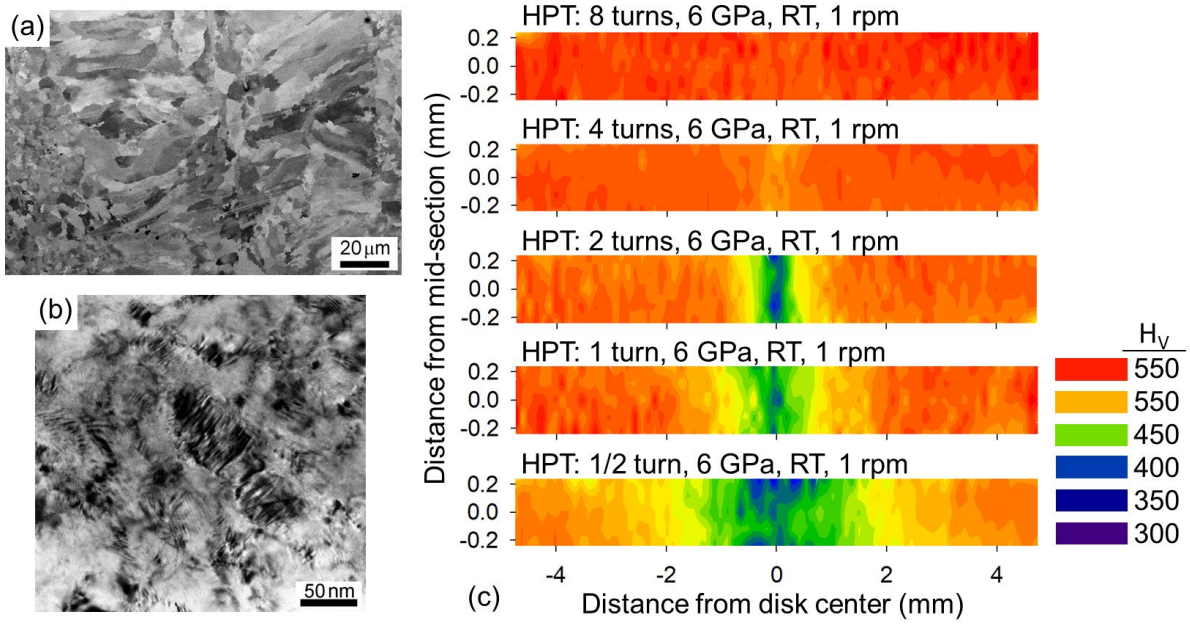

Figure 1. Micrographs of the alloy (a) in as-built and (b) after HPT for 8 turns, and (c) color-coded hardness contour maps after HPT for 1/2 turn through 8 turns of AM CoCrFeNi alloy.

A series of samples including AM powder before AM, after AM (as-built), and after HPT for 1/2 turn through 8 turns were examined by the X-ray diffraction (XRD) method. All sample conditions showed diffraction peaks of only face-centered cubic (f.c.c.) structure, and the estimated microstructure parameters including crystallite size, microstrain, and lattice constant are listed in Table 1 [5]. While there is a slight change before and after AM, significant changes in these microstructural parameters are initiated by the application of HPT even for 1/2 turn. The changes in the parameters are maintained reasonably through 8 turns. It is common to observe a smaller domain size of 75 nm by XRD after 8 turns than by TEM (Fig. 1(b)) due to the high populations of subgrains and dislocation walls as well as crystallographic orientation [7].

Table 1. Summary of estimated crystallite size, microstrain, and lattice parameters for the AM CoCrFeNi alloy in the conditions of powder, after AM, and HPT for up to 8 turns [5].

	Crystallite size (nm)	Microstrain	Lattice constant (Å)
Powder	462.54	0.00495	3.5718 ± 0.0007
As-built	652.27	0.00410	3.5744 ± 0.0009
HPT: 1/2 turn	101.25	0.00810	3.5742 ± 0.0048
HPT: 1 turn	116.11	0.00881	3.5728 ± 0.0051
HPT: 2 turns	80.94	0.00858	3.5752 ± 0.0059
HPT: 4 turns	89.65	0.00878	3.5745 ± 0.0059
HPT: 8 turns	75.07	0.00834	3.5771 ± 0.0069

In-situ heating neutron diffraction analysis

Microstructural evolution upon heating at 4 K/min from 300 K to 1273 K followed by quenching was examined for the as-built and HPT-processed CoCrFeNi alloy through neutron diffraction experiments at the iMATERIA, beamline BL20, at the Japan Proton Accelerator Research Complex (J-PARC) [8]. The obtained time-resolved neutron diffraction patterns from Banks 1-3 are plotted into diffraction contour maps with temperature changes as shown in Fig. 2 for the CoCrFeNi alloy in (a) as-built and (b) AM and HPT for 15 turns [8]. HPT for 15 turns was applied to ensure the homogeneous nanostructure of the alloy. The peak profiles at t = 0 min of heating imply the textures of the alloy conditions immediately after AM (a) and HPT (b).

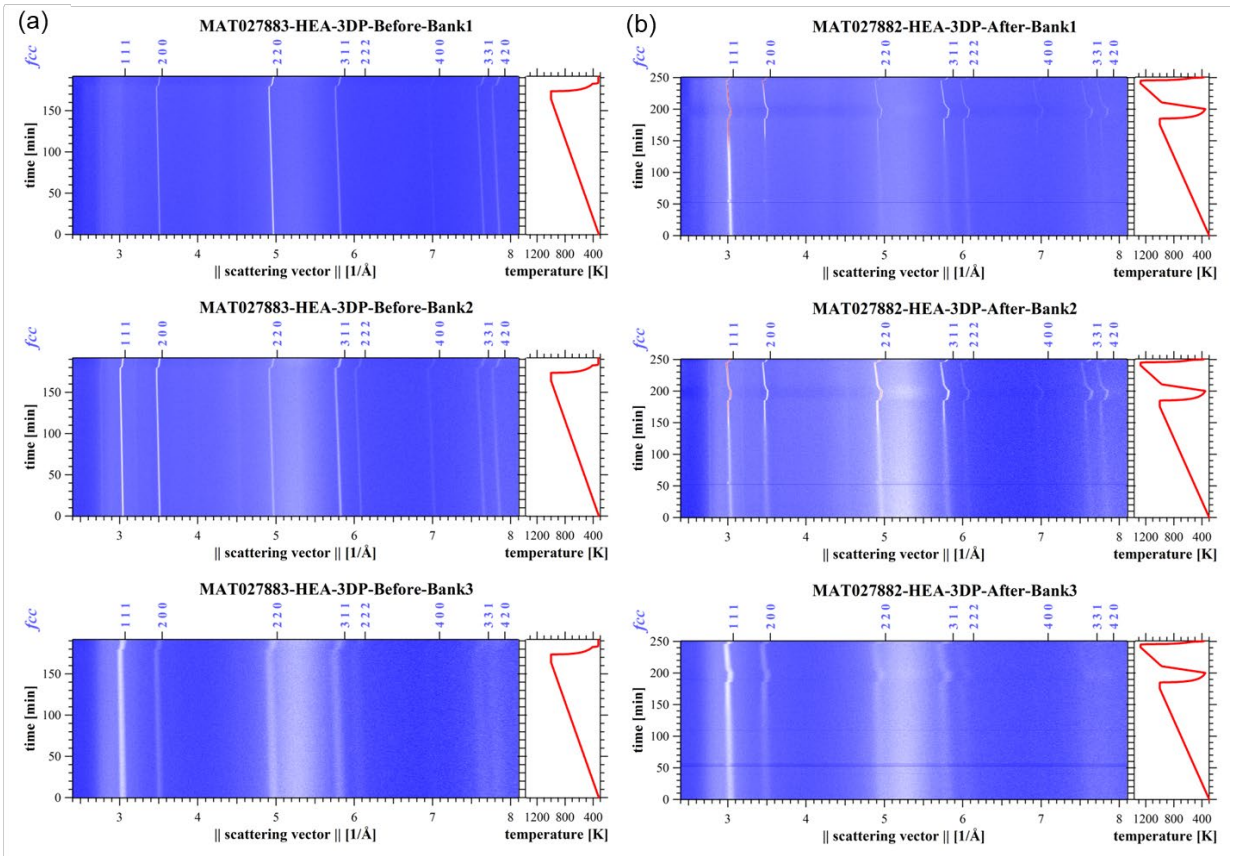

Figure 2. Contour plots showing variation in neutron diffraction profiles from three detector banks 1-3 with time and temperature for the AM CoCrFeNi HEA after (a) printing and (b) HPT for 15 turns [8].

Materials Research Proceedings **32** (2023) 235-243 https://doi.org/10.21741/9781644902615-27

Both materials showed diffraction peaks of a single-phase f.c.c. crystal structure throughout heating followed by cooling, thereby proving no phase transformation. In addition, two features are noticeable in the contour plots of neutron diffraction profiles with time and temperature for the CoCrFeNi alloy: the continuous and concurrent changes in the peak shifting and peak width. The former indicates lattice expansion and contraction with heating and cooling, respectively, and the latter involves relaxation in microstrain and growth in crystallite size, indicating microstructural relaxation. These parameters are further analyzed, and Fig. 3 shows the evolution of (a) peak lattice expansion and (b) relative peak width at the plane coordinate of 111 of the neutron diffraction peaks with temperature for both as-built (AM) and HPT-processed (AM + HPT) CoCrFeNi alloy [8]. The relative lattice expansion and contraction in Fig. 3(a) were estimated using the base lattice parameter of a_0 = 3.60 Å taken at the minimum strain condition after the completion of a heating-cooling cycle in the diffraction measurement. Ex-situ hardness measurements after heating to the specific target temperatures followed by cooling were conducted for the samples, where the results are shown in Fig. 3(c).

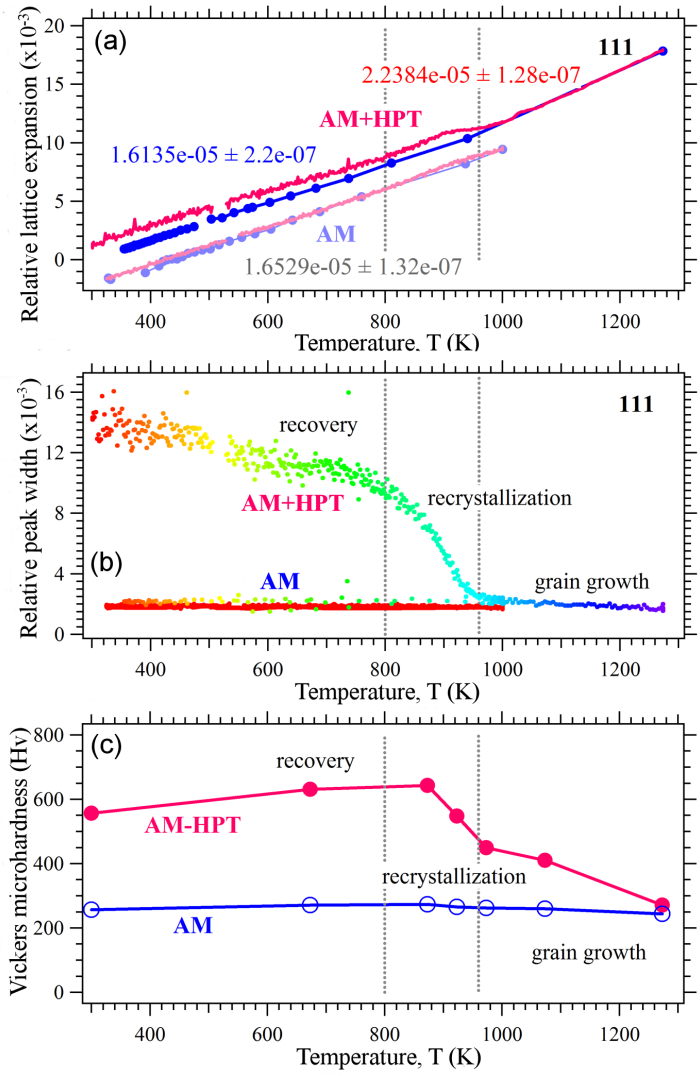

Figure 3. Evolution of (a) relative peak width, (b) relative lattice expansion, and (c) Vickers microhardness upon heating for the as-printed (AM) and HPT-processed (AM + HPT) CoCrFeNi alloy [8].

Materials Research Proceedings **32** (2023) 235-243 https://doi.org/10.21741/9781644902615-27

For both AM and AM + HPT samples, there is a consistent linear lattice contraction of ~1.6×10^{-5} K^{-1} at <900 K, while a high lattice expansion of 2.2×10^{-5} K^{-1} is observed over 960 K with some plateau at 900-960 K for AM + HPT. Such inconsistency in relative lattice expansion without phase transformation can be explained by the inhomogeneous distribution of thermal vacancies leading to heterogeneous lattice strain in CoCrFeNi and CoCrFeNiMn high-entropy alloys at >973 K [9]. The changes in relative peak width and hardness values with heating towards 1273 K in Fig. 3(b) and (c) provide microstructural relaxation behavior of the nanostructured CoCrFeNi alloy, which are not visible in the AM sample. In practice, the gradual reduction in relative peak width and a hardness increase from H_V of 550 to 650 are shown up to 873 K, followed by a dramatic decrease in both relative peak width and hardness to $H_V \approx 450$ through 973 K, and these achieved the minimum saturated values of peak width and hardness of $H_V \approx 370$ with further heating thought 1273 K. These three stages of microstructural relaxation are considered as recovery, recrystallization, and grain growth.

Annealing-induced hardening (AH) [10] is achieved upon heating to 873 K in the present UFG CoCrFeNi alloy. AH has been observed in other SPD-processed UFG metals, including stainless steel [11], single-phase CoCrNi-based medium entropy alloys [12], Ni-Mo alloy [13], and Ti [14]. AH must be differentiated from transformation hardening, including the nucleation of Guinier-Preston zones in Al alloys and the formation of NiMn-, FeCo-, and Cr-rich phases in the CoCrFeNiMn Cantor alloy. Moreover, AH is achievable without solute segregation strengthening [15]. Specifically, UFG metals processed through a top-down strategy, such as SPD, achieved AH by defect relaxation involving (i) relaxation of mobile dislocations inside the grains by clustering into low energy configurations without any significant loss in dislocation density; (ii) relaxation of non-equilibrium grain boundaries leading to a difficult emission of dislocations; and (iii) clustering of excess vacancies into planer defects, impeding the motion of dislocations. The ductility of UFG metals after AH is anticipated to be improved because of the microstructural relaxation during annealing. Accordingly, the AH effect on the UFG metals differs from the “yield strength anomaly”, which strengthens materials at elevated temperatures by dislocation locking and dynamic strain aging strengthening leading to lower ductility [16].

The in-situ neutron diffraction experiments provide a knowledge base to minutely design crystalline microstructures and improve the desired properties of a UFG material by an accurate post-processing heating treatment. A recent report summarized currently available examples of SPD-processed nanostructured materials which are characterized by synchrotron X-ray and neutron diffraction techniques [17].

In-situ heating laser scanning confocal microscopy

The present neutron diffraction analysis as well as lab-scale X-ray and synchrotron diffraction analyses can capture the non-monotonous distribution of diffraction peak broadening, indicating strain anisotropy, due to the heterogeneous distributions of excess numbers of dislocations, vacancies, and other defects within crystals of SPD-processed metals [18]. The microstructural inhomogeneity and heterogeneous evolution of a UFG microstructure can be observed by microscopy techniques that are capable of scanning over large-length scales. A recent experiment demonstrated a heterogeneous microstructural relaxation behavior of an HPT-processed nanocrystalline CoCrFeNiMn alloy having saturated grain sizes of 40-50 nm through laser scanning confocal microscopy (LSCM) (Model VL2000DX-SVF18SP) with a heating facility [17]. The principles of LSCM including how the observed surface information represents the bulk behavior of materials are explained elsewhere [19]. Figure 4 shows a series of the LSCM micrographs taken at cross-sections of the alloy disk edges upon heating from 373 K to 923 K at 10 K/min.

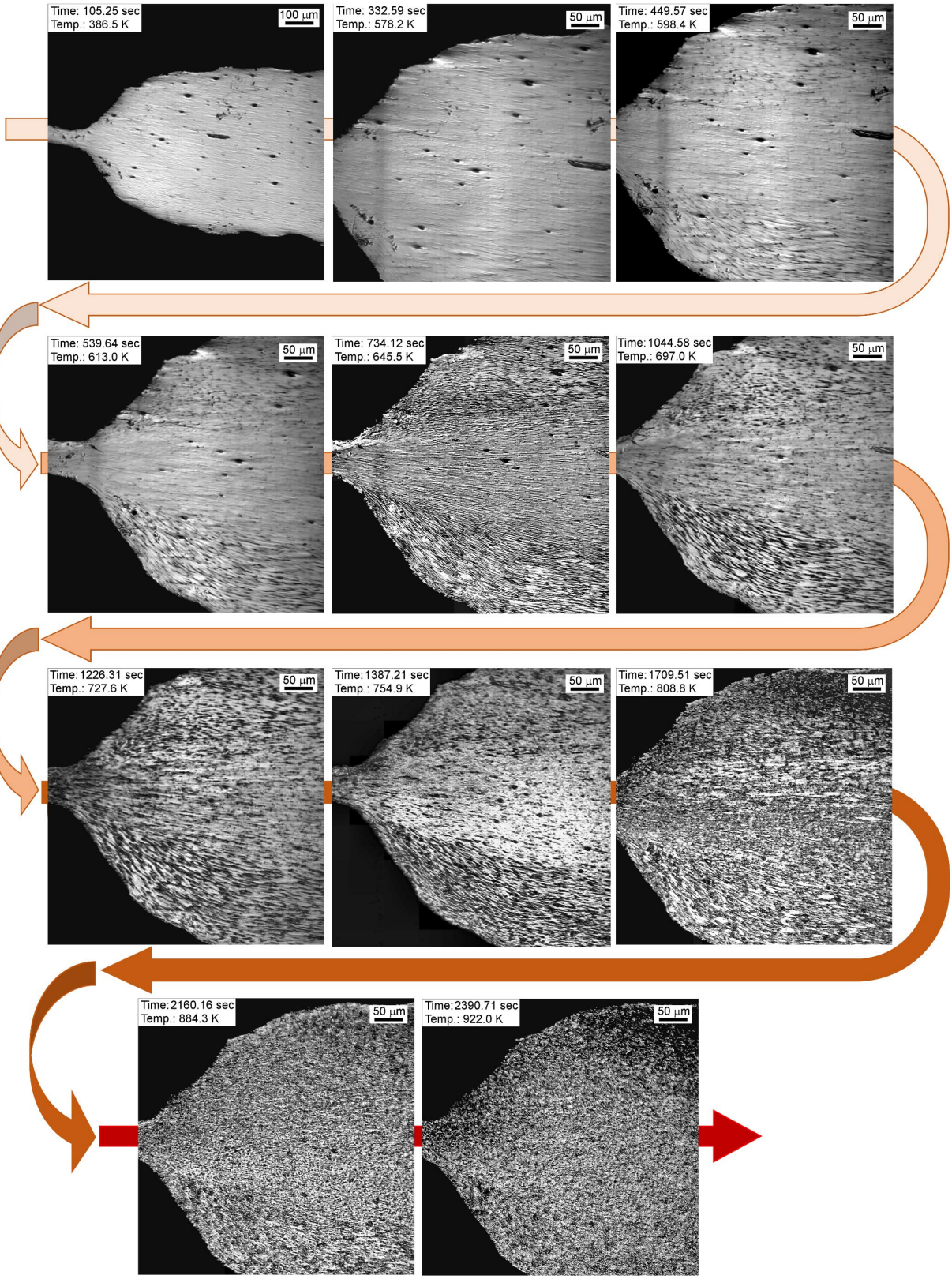

Figure 4. A series of LSCM micrographs taken at a disk edge region of the HPT-processed CoCrFeNiMn HEA at arbitrarily selected temperatures between 373 K and 923 K. The micrographs are adopted from [17].

Overall homogeneous microstructure until 580 K started to show coarser multi-phase elongated phases aligning shear directions only at the sample surfaces except for the middle-thickness without coarsening through 650 K. The separated phase evolution with phase coarsening was maintained until 800 K. Above this temperature, all regions are coarsened, and the equiaxed phases are homogeneously distributed across the sample thickness. While it is a preliminary result without characterization of the coarsened phases, the heterogeneous microstructure evolution during heating was visualized within the HPT-processed CoCrFeNiMn HEA disk sample by the application of high-temperature LSCM for the first time. The phase transformation and agglomerations of the nanostructured CoCrFeNiMn alloy were observed at 723 K [20], but careful consideration is required for the local measurements for microstructural analysis and small-scale mechanical testing, i.e. nanoindentation, due to the possible heterogeneous microstructure and texture introduced by SPD processing. These diffraction and microscopy techniques which analyze the large sample volumes and areas are essential and complementary to the other local measurements to fully understand the evolution of microstructure and mechanical properties of the SPD-processed UFG metals.

Summary

The novel characterization techniques of in-situ heating neutron diffraction and high-temperature laser scanning confocal microscopy provided a comprehensive view of the continuous microstructural relaxation of bulk nanocrystalline HEAs. With the application of different techniques, the heterogeneous UFG microstructures developed during heating can be revealed and understood precisely.

Acknowledgments

This study was supported in part by the National Science Foundation of the United States under Grant No. CMMI-2051205 (M.K.). The authors greatly acknowledge the Ibaraki prefectural government and the J-PARC facility for granting access to iMATERIA under the 2019 Overseas Academic User Program of Ibaraki Neutron Beamline BL20, proposal number 2019PM2014. The authors acknowledge the University of Wollongong for granting access to facilities in the High-temperature Microscopy Laboratory.

References

[1] A. Kumpmann, B. Gunther, H.D. Kunze, Thermal-stability of ultrafine-grained metals and alloys, Mater. Sci. Eng. A 168 (1993) 165-169. https://doi.org/10.1016/0921-5093(93)90722-Q

[2] C.C. Koch, R.O. Scattergood, K.A. Darling, J.E. Semones, Stabilization of nanocrystalline grain sizes by solute additions, J. Mater. Sci. 43 (2008) 7264-7272. https://doi.org/10.1007/s10853-008-2870-0

[3] D.-H. Lee, I.-C. Choi, M.-Y. Seok, J. He, Z. Lu, J.-Y. Suh, M. Kawasaki, T.G. Langdon, J.-i. Jang, Nanomechanical behavior and structural stability of a nanocrystalline CoCrFeNiMn high-entropy alloy processed by high-pressure torsion, J. Mater. Res. 30 (2015) 2804-2815. https://doi.org/10.1557/jmr.2015.239

[4] Y. Kuzminova, D. Firsov, A. Dudin, S. Sergeev, A. Zhilyaev, A. Dyakov, A. Chupeeva, A. Alekseev, D. Martynov, I. Akhatov, S. Evlashin, The effect of the parameters of the powder bed fusion process on the microstructure and mechanical properties of CrFeCoNi medium-entropy alloys, Intermetallics 116 (2020) 106651. https://doi.org/10.1016/j.intermet.2019.106651

[5] W. Zhao, J.-K. Han, Y.O. Kuzminova, S.A. Evlashin, A.P. Zhilyaev, A.M. Pesin, J.-i. Jang, K.-D. Liss, M. Kawasaki, Significance of grain refinement on micro-mechanical properties and

structures of additively-manufactured CoCrFeNi high-entropy alloy, Mater. Sci. Eng. A 807 (2021) 140898. https://doi.org/10.1016/j.msea.2021.140898

[6] A.P. Zhilyaev, T.G. Langdon, Using high-pressure torsion for metal processing: Fundamentals and applications, Prog. Mater. Sci. 53 (2008) 893-979. https://doi.org/10.1016/j.pmatsci.2008.03.002

[7] J. Gubicza, P.T. Hung, M. Kawasaki, J.-K. Han, Y. Zhao, Y. Xue, J.L. Lábár, Influence of severe plastic deformation on the microstructure and hardness of a CoCrFeNi high-entropy alloy: A comparison with CoCrFeNiMn, Mater. Charact. 154 (2019) 304-314. https://doi.org/10.1016/j.matchar.2019.06.015

[8] X. Liu, J.-K. Han, Y. Onuki, Y.O. Kuzminova, S.A. Evlashin, M. Kawasaki, K.-D. Liss, In situ neutron diffraction investigating microstructure and texture evolution upon heating of nanostructured CoCrFeNi high-entropy alloy, Adv. Eng. Mater. 25 (2023) 2201256. https://doi.org/10.1002/adem.202201256

[9] E.W. Huang, H.-S. Chou, K.N. Tu, W.-S. Hung, T.-N. Lam, C.-W. Tsai, C.-Y. Chiang, B.-H. Lin, A.-C. Yeh, S.-H. Chang, Y.-J. Chang, J.-J. Yang, X.-Y. Li, C.-S. Ku, K. An, Y.-W. Chang, Y.-L. Jao, Element effects on high-entropy alloy vacancy and heterogeneous lattice distortion subjected to quasi-equilibrium heating, Sci. Rep. 9 (2019) 14788. https://doi.org/10.1038/s41598-019-51297-4

[10] J. Gubicza, Annealing-induced hardening in ultrafine-grained and nanocrystalline materials, Adv. Eng. Mater. 22 (2020) 1900507. https://doi.org/10.1002/adem.201900507

[11] M. Kawasaki, J.-K. Han, X. Liu, Y. Onuki, Y.O. Kuzminova, S.A. Evlashin, A.M. Pesin, A.P. Zhilyaev, K.-D. Liss, In situ heating neutron and X-ray diffraction analyses for revealing structural evolution during post-printing treatments of additive-manufactured 316L stainless steel, Adv. Eng. Mater. 24 (2021) 2100968. https://doi.org/10.1002/adem.202100968

[12] P.T. Hung, M. Kawasaki, J.K. Han, A. Szabo, J.L. Labar, Z. Hegedus, J. Gubicza, Thermal stability of nanocrystalline CoCrFeNi multi-principal element alloy: Effect of the degree of severe plastic deformation, Intermetallics 142 (2022) 107445. https://doi.org/10.1016/j.intermet.2021.107445

[13] J. Gubicza, P.H.R. Pereira, G. Kapoor, Y. Huang, S.S. Vadlamani, T.G. Langdon, Annealing-induced hardening in ultrafine-grained Ni-Mo alloys, Adv. Eng. Mater. 20 (2018) 1800184. https://doi.org/10.1002/adem.201800184

[14] R.Z. Valiev, A.V. Sergueeva, A.K. Mukherjee, The effect of annealing on tensile deformation behavior of nanostructured SPD titanium, Scr. Mater. 49 (2003) 669-674. https://doi.org/10.1016/S1359-6462(03)00395-6

[15] O. Renk, A. Hohenwarter, K. Eder, K.S. Kormout, J.M. Cairney, R. Pippan, Increasing the strength of nanocrystalline steels by annealing: Is segregation necessary?, Scr. Mater. 95 (2015) 27-30. https://doi.org/10.1016/j.scriptamat.2014.09.023

[16] H. Shang, Q. Ma, Q. Gao, H. Zhang, H. Li, H. Zhang, L. Sun, Yield strength anomaly evaluation of W-free Co-Ni-Al-based superalloys during high temperature tensile tests, Mater. Charact. 192 (2022) 112242. https://doi.org/10.1016/j.matchar.2022.112242

[17] M. Kawasaki, J.-K. Han, X. Liu, S.-C. Moon, K.-D. Liss, Synchrotron high-energy X-ray & neutron diffraction, and laser-scanning confocal microscopy: in-situ characterization techniques for bulk nanocrystalline metals, Mater. Trans. (2023) in press. https://doi.org/10.2320/matertrans.MT-MF2022022

[18] T. Ungár, Characterization of nanocrystalline materials by X-ray line profile analysis, J. Mater. Sci. 42 (2006) 1584-1593. https://doi.org/10.1007/s10853-006-0696-1

[19] S.-C. Moon, D. Phelan, R. Dippenaar, New insights of the peritectic phase transition in steel through in-situ measurement of thermal response in a high-temperature confocal microscope, Mater. Charact. 172 (2021) 110841. https://doi.org/10.1016/j.matchar.2020.110841

[20] D.H. Lee, J.A. Lee, Y.K. Zhao, Z.P. Lu, J.Y. Suh, J.Y. Kim, U. Ramamurty, M. Kawasaki, T.G. Langdon, J.I. Jang, Annealing effect on plastic flow in nanocrystalline CoCrFeMnNi high-entropy alloy: A nanomechanical analysis, Acta Mater. 140 (2017) 443-451. https://doi.org/10.1016/j.actamat.2017.08.057